Modeling of Growth Rate Dispersion in Batch Cooling Crystallization

Martin Bohlin and Åke C. Rasmuson
Dept. of Chemical Engineering, Royal Institute of Technology, S-100 44 Stockholm, Sweden

The influence of growth rate dispersion on the product-size distribution of batch cooling crystallization is investigated by computer simulations. The model accounts for primary and magma density-dependent secondary nucleation, and growth rate dispersion of the constant crystal growth type. The model is solved by a combination of the method of characteristics and moment analysis, by which the entire product-size distribution is recovered. The study includes three different growth rate activity distributions, and the influence of the corresponding coefficient of variation is analyzed for unseeded and seeded processes. The results show that the effect of growth rate dispersion on the crystal-size distribution may be significant even at moderate dispersion. At high dispersion, even the actual shape of the growth rate activity distribution may become important.

Introduction

Modeling of batch crystallizers has increased the understanding of the interaction of crystal growth and nucleation via the supersaturation, and the influence of process conditions on the final product-size distribution (Tavare, 1987; Bohlin and Rasmuson, 1992). However, further development of models and methods of determination of kinetics is needed for successful prediction of the performance of real crystallizers. In recent years, the concept of growth rate dispersion has been increasingly recognized as an important feature of crystal growth. Growth rate dispersion implies that crystals of the same size and shape grow at different rates in the same environment. Two different types of growth rate dispersion (GRD) are discussed. Randolph and White (1977) suggested that the growth rate of an individual crystal randomly fluctuates about a mean value during the growth period (random fluctuation model, RF). Alternatively, each individual crystal possesses a certain growth rate, but a distribution of growth rates exists among the crystals in the suspension (constant crystal growth model, CCG) (Janse and de Jong, 1976; Ramanarayanan et al., 1985). Human et al. (1982) observed a high dispersion of the growth rate in time, and results of Tulke and Offermann (1990) also indicate random fluctuations. However, the CCG behavior is reported more often (all references in Table 1; Berglund et al., 1983; Mathis-Lilley and Berglund, 1985). Experimentally-determined values of the growth rate coefficient of variation, CV_G, for different substances are collected in Table 1. Obviously, the spread of growth rates may be significant.

The influence of growth rate dispersion in continuous crystallization has been analyzed by several authors, and equations for the complete product-size distribution have been presented [Berglund and Larson, 1984 (CCG); Larson et al., 1985 (CCG); Rousseau and Zumstein, 1986 (CCG and RF); Gupta and Dutta, 1990 (CCG and RF)]. For batch crystallization, most work has been devoted to isothermal processes (constant supersaturation or no supersaturation generation) and prediction of the mean and variance or coefficient of variation (CV) of the product-size distribution as a function of time [Randolph and White, 1977 (RF); Melikhov and Berliner, 1981 (RF); Tavare and Garside, 1982 (RF); Berglund and Murphy, 1986 (CCG and RF); Rousseau and Zumstein, 1986 (CCG and RF)]. Ramanarayanan et al. (1984) analyzes how the moments of a certain population of crystals evolves at constant supersaturation assuming the CCG model, using a mathematical-statistical approach. The moments of the product-size distribution are expressed in terms of the moments of the growth rate distribution. Using a slightly different approach, Klug and Pigford (1989) extend these results for the case of changing supersaturation. Shiau and Berglund (1990) (CCG-model) present an extended moment analysis in which also further nucleation is allowed. Lakatos et al. (1984) model random fluctuations in a batch crystallizer and solve for the complete population den-

Correspondence concerning this article should be addressed to Å. C. Rasmuson.

Table 1. Experimental Values of Growth Rate Dispersion for Some Substances

Substance	CV_G	Comment	Reference
Potassium dichromate	27-100%	Seed crystals	Janse, de Jong (1979)
ADP	37-44%	Primary nucleation	Garside, Ristic (1983)
ADP	42-100%	Secondary nuclei (contact nuclei)	Blem, Ramanarayanan (1987)
Fructose	20-30%	Contact nuclei	Shiau, Berglund (1987)
Sucrose	36%	Secondary nuclei (contact nuclei)	Liang et al. (1987a)
Sucrose	36%	Seed crystals *and* contact nuclei	Liang et al. (1987b)
Sucrose	43-55%	Seed crystals	Berglund, Murphy (1986)
Potash Alum	49%	Initial breeding	Zumstein, Rousseau (1987)
Potash Alum	17-30%	Seed crystals	Janse, de Jong (1979)
Sodium Sulphate	21-42%	Seed crystals	Klug, Pigford (1989)
Sodium Sulphate	35-85%	Secondary nuclei	Klug, Pigford (1989)
Citric Acid	30-78%	Contact nucleation	Ramanarayanan et al. (1985)

sity distribution by orthogonal collocation, but very few results are presented. Janse (1977) and de Jong (1986) use a simulation method based on the method of characteristics. The evolution of pulses of nuclei and seeds through the size range is recorded. Each new pulse is discretized into subgroups of different growth rates (CCG model), and the complete size distribution is calculated.

This article aims at elucidating the importance of growth rate dispersion on the product properties of a batch cooling crystallization. By computer simulations, the influence of the coefficient of variation and the functional shape of the growth rate distribution are analyzed. The model accounts for primary nucleation, magma density-dependent secondary nucleation and growth rate dispersion of the CCG type. The method of solution recovers the complete product-size distribution. Citric acid monohydrate is used as a model substance. Early experimental results on this substance were interpreted as size-dependent growth (Sikdar and Randolph, 1976; Laguerie and Angelino, 1979), but it has later been shown convincingly that growth rate dispersion dominates and can be described by the CCG model (Berglund, 1981; Berglund and Larson, 1982, 1984; Ramanarayanan et al., 1985). The reported spread of the growth rates for citric acid monohydrate, CV_G, varies between 30 and 78%.

Model

The population balance for a batch cooling crystallization is derived assuming that (i) the crystallizer is well-mixed, (ii) crystal breakage and agglomeration are negligible, (iii) crystal growth is independent of size, (iv) there is no growth rate dispersion, and (v) crystals are born at zero size:

$$\frac{\partial n}{\partial t} + G\frac{\partial n}{\partial L} = 0 \tag{1}$$

This equation can be solved by the method of characteristics as was recently done by Bohlin and Rasmuson (1992), Qiu and Rasmuson (1991), Jager et al. (1991), and Kramer et al. (1990). In the case of growth rate dispersion according to the CCG model, Klug and Pigford (1989) define the growth rate of each crystal as:

$$G = \frac{dL}{dt} = k_g \cdot D[\Delta c(t),\ T(t)] \tag{2}$$

The distribution of k_g values is described by the distribution function P_g:

$$P_g = P_g(\bar{k}_g, \sigma_g, k_g) \tag{3}$$

We call k_g the growth rate activity and assume that the specific value of each crystal is received at birth and is retained unchanged with size, temperature, and supersaturation. For this case, Eq. 1 has to be formulated for each value of k_g,

$$\frac{\partial n(L,t;k_g)}{\partial t} + k_g \cdot D(\Delta c, T) \cdot \frac{\partial n(L,t;k_g)}{\partial L} = 0 \tag{4}$$

and the total population density becomes:

$$n(L,t) = \int_0^\infty n(L,t;k_g)\,dk_g \tag{5}$$

On these two equations, Klug and Pigford (1989) based the derivation of equations for the evolution of the moments of a defined population of crystals, seeded or primary nucleated, having a distribution of growth rates. The moments of the size distribution are expressed in terms of the moments of the growth rate distribution and the extent of growth. In this work, the method of characteristics is combined with this moment analysis, and the complete size distribution is recovered without discretizing the growth rate distribution.

Besides the above-mentioned assumptions i-iii and v, it is assumed that (vi) the crystal shape is constant regardless of size and time and that (vii) growth rate dispersion is of the CCG type (no random fluctuations). Simulation of crystallization of citric acid monohydrate is performed, and the equations are thus formulated using variables expressing total amounts in the crystallizer ($\tilde{N} = N \cdot M$, $\tilde{m} = m \cdot M$, and so on). The solution algorithm discretizes the crystal generation process into "pulses" of particles. Using the method of characteristics, these pulses are traced as they move along the size axis at the rate of crystal growth, $G(t)$ (Randolph and Larson, 1988). Crystals born over a time interval, Δt, are collected in one pulse, and the number of crystals in the pulse, $\tilde{N}_i$, is the integral of the total nucleation rate over the interval:

$$\tilde{N}_i = \int_{t_i}^{t_i + \Delta t} [B_p + B_s] \cdot M\,dt \tag{6}$$

where t_i is the "birth time" of pulse i, and $t_1 = 0$. In each time interval, one new pulse is born. The primary and secondary nucleation rates are described by power laws:

$$B_p = k_p \cdot \Delta c^{n_p} \tag{7}$$

$$B_s = k_s(T) \cdot W_T^b \cdot \Delta c^{n_s} \tag{8}$$

Seeds are added at $t = 0$, and receive $i = 0$. It is assumed that both the seed pulse and the nuclei pulses are initially monosized, but there is a distribution of growth rate activity (Eq. 3) within the pulses. At growth conditions, the mean size and width increase, but the resulting subpopulation distribution retains a constant functional shape equal to the functional shape of the growth rate distribution, P_g (Ramanarayanan et al., 1984). For each subpopulation, we use moment analysis to determine the evolution of its mean size, width and mass as a function of time. The jth moment of the size distribution of the ith subpopulation, $\tilde{m}_{Lji}$, is calculated from the moments of the initial size distribution of the subpopulation, the moments of the growth rate activity distribution, m_{gr}, and the transformed time, Θ_i. The result can be summarized as (Ramanarayanan et al., 1984; Klug and Pigford, 1989):

$$\tilde{m}_{Lji}(\Theta_i) = \sum_{r=0}^{r=j} \binom{j}{r} \tilde{m}_{L(j-r)i}(0) \cdot m_{gr} \cdot \Theta_i^r \tag{9}$$

The transformed time of the ith subpopulation at time t, $\Theta_i(t)$, is defined as the integral of the driving force function, D, from the commencement of growth of the particular population, t_{i+1}, to time t:

$$\Theta_i = \int_{t_{i+1}}^{t} D(\Delta c, T)\, dt \tag{10}$$

For the seed pulse, $t_{i+1} t_1 = 0$. The initial moments of the subpopulations are defined as:

$$\tilde{m}_{Lji}(\Theta_i = 0) = \tilde{N}_i \cdot (L_{i0})^j \tag{11}$$

which for zero size nuclei reduces to:

$$\begin{aligned} \tilde{m}_{L0i}(\Theta_i = 0) &= \tilde{N}_i \\ \tilde{m}_{Lji}(\Theta_i = 0) &= 0 \quad j > 0 \end{aligned} \tag{12}$$

For the determination of the size distribution of each subpopulation, Eq. 17, the corresponding first three moments ($r = 0$, 1, 2) need to be calculated by Eq. 9. This allows for a complete description of the total size distribution by Eq. 16. By calculation of the third moment ($r = 3$) of each subpopulation, the computation of the total mass by Eq. 15 is allowed for, which is much more efficient than an integration of Eq. 16. As discussed later, the mean size and the variance of the total distribution can be efficiently calculated by Eqs. 22–25, if also two additional moments ($r = 4$, 5) of the subpopulations are known. To calculate the first six moments of the subpopulations, the first six moments of the growth activity distribution are needed, as given in the Appendix.

The population balance is coupled to the supersaturation balance and the solvent mass balance by the third moment of the total size distribution:

$$\frac{d(M \cdot \Delta c)}{dt} = -\frac{d(M \cdot c^*)}{dt} - \frac{d(\tilde{W}_T/R)}{dt}; \quad \Delta c(t=0) = \Delta c_o \tag{13}$$

$$\frac{dM}{dt} = -\frac{d\tilde{W}_T}{dt} \cdot \left[\frac{R-1}{R}\right]; \quad M(t=0) = M_o \tag{14}$$

and

$$\tilde{W}_T(t) = k_v \cdot \rho_c \cdot \tilde{m}_{L3}(t) = k_v \cdot \rho_c \cdot \sum_{i=0}^{k} \tilde{m}_{L3i}[\Theta_i(t)] \tag{15}$$

since the total mass is the sum of the mass of all subpopulations. The temperature in the crystallizer is given explicitly by the adopted temperature profile. The system of Eqs. 6–15 is solved by Euler's method. In each time step, Eqs. 6 and 10 are solved for the nucleation rate, $\tilde{N}_i$, and the transformed times, Θ_i. Then, the change of the crystal size and mass is calculated by using Eq. 9. Finally, the mass and solvent balances, Eqs. 13 and 14, are solved simultaneously for the solute concentration and solvent mass. Time steps of 40 seconds are acceptable for the calculations of this study. Further refinement of the time steps does not change the results significantly.

The total population density at size L is the sum of the population densities of the subpopulations at size L:

$$\tilde{n}(L) = \sum_{i=0}^{k} \tilde{n}_i(L) \tag{16}$$

The population density distribution of the subpopulation, $\tilde{n}_i(L)$, has a functional form dictated by the growth distribution function and is basically constructed by taking the growth rate activity function, Eq. 3, changing the parameters, $\bar{k}_g$ and σ_g to size variables $\bar{L}_i$ and σ_{Li} and finally multiplying with the total number of crystals in the subpopulation $\tilde{N}_i$:

$$\tilde{n}_i(L) = \tilde{N}_i \cdot P_{Li}(\bar{L}_i, \sigma_{Li}, L) \tag{17}$$

The population density distributions corresponding to three different growth rate distributions, a normal, a log-normal and a gamma distribution, are given in the Appendix.

The mean size and variance of the subpopulation are calculated by Eqs. 18 and 19 (Randolph and Larson, 1988):

$$\bar{L}_i = \frac{\tilde{m}_{L1i}}{\tilde{m}_{L0i}} = \frac{\tilde{m}_{L1i}}{\tilde{N}_i} \tag{18}$$

$$\sigma_{Li}^2 = \frac{\tilde{m}_{L2i}}{\tilde{m}_{L0i}} - \frac{\tilde{m}_{L1i}^2}{\tilde{m}_{L0i}^2} = \frac{\tilde{m}_{L2i}}{\tilde{N}_i} - \frac{\tilde{m}_{L1i}^2}{\tilde{N}_i^2} \tag{19}$$

using the result of Eq. 9. The total population density distribution is normally calculated with a resolution of 10–20 μm. In the diagrams, all population densities are converted to "^{10}log no/kg water, m" by dividing with the mass of free solvent, $M(t)$. The cumulative undersize mass distribution is calculated by numerical integration of the third moment, to size L:

Table 2. Numerical Values of Parameters Used in the Simulations

Parameter	Value	Ref.	Parameter	Value	Ref.
Batch time, t_f	12,000		Density of crystals, ρ_c	1,540	1
Start temperature, θ_o	35		Volume shape factor, k_v	0.52	4
Final temperature, θ_f	20		Hydrate factor, R	1.0938	
Initial solvent mass, M_o	1.0		Primary nucl. order, n_p	3.54	2
Initial supersat., Δc_o	0.0		Primary nucl. const., k_p	1.0×10^{8}	2
Number of seeds, N_s	10^6		Secondary nucl. const., k_s	$0.5\times\exp(4781/T)$	3,4
Initial size of seeds, L_{so}	0.2×10^{-3}		Secondary nucleation order, n_s	0.543	3,4
Solubility constants,* c_o	0.91176	1	Mass exponent, b	0.84	3,4
Solubility constants,* c_1	3.4857×10^{-2}	1	Mean growth activity, $\bar{k}_g$	0.02652	3,4
Solubility constants,* c_2	-2.8785×10^{-4}	1	Driving force function, D	$\exp(-3{,}584/T)\cdot\Delta c^g$	3,4
Solubility constants,* c_3	3.7228×10^{-6}	1	Growth rate order, g	0.65	3,4

*Third-order polynomial fit to published data: $c^* = c_o + c_1\cdot\theta + c_2\cdot\theta^2 + c_3\cdot\theta^3$.
References: 1. Mullin (1972); 2. Nyvlt et al. (1985); 3. Sikdar and Randolph (1976); 4. Mukhopadhyay and Epstein (1980).

$$m_{\text{cum}}(L) = \frac{k_v\cdot\rho_c\cdot\int_0^L \tilde{n}(L)\cdot L^3 dL}{k_v\cdot\rho_c\cdot\int_0^\infty \tilde{n}(L)\cdot L^3 dL} = \frac{k_v\cdot\rho_c\cdot\int_0^L \tilde{n}(L)\cdot L^3 dL}{\tilde{W}_T} \tag{20}$$

The moments of the total distribution are obtained by inserting Eq. 16 into the moment definitions. It is then immediately observed that each moment can be determined by simply summing up the corresponding moments of all subpopulations:

$$\tilde{m}_{Lj} = \sum_{i=0}^{k} \tilde{m}_{Lji} \tag{21}$$

Thus, the mean size and the variance of the total distribution are calculated directly from the moments of the subpopulations by:

$$\bar{L}_{nd} = \sum_{i=0}^{k} \tilde{m}_{L1i} \Big/ \sum_{i=0}^{k} \tilde{m}_{L0i} \tag{22}$$

$$\bar{L}_{wd} = \sum_{i=0}^{k} \tilde{m}_{L4i} \Big/ \sum_{i=0}^{k} \tilde{m}_{L3i} \tag{23}$$

$$\sigma^2_{nd} = \frac{\sum_{i=0}^{k} \tilde{m}_{L2i}}{\sum_{i=0}^{k} \tilde{m}_{L0i}} - \left[\frac{\sum_{i=0}^{k} \tilde{m}_{L1i}}{\sum_{i=0}^{k} \tilde{m}_{L0i}}\right]^2 \tag{24}$$

$$\sigma^2_{wd} = \frac{\sum_{i=0}^{k} \tilde{m}_{L5i}}{\sum_{i=0}^{k} \tilde{m}_{L3i}} - \left[\frac{\sum_{i=0}^{k} \tilde{m}_{L4i}}{\sum_{i=0}^{k} \tilde{m}_{L3i}}\right]^2 \tag{25}$$

Of course, the moments of the total distribution can be calculated by inserting Eq. 16 into the definitions of the moments and perform the integrations. However, these calculations extend the total simulation time significantly. Four to five times more computer time is required to reach an accuracy of the numerical integration that reduces the error in mean sizes and coefficient of variations (CV_{nd} and CV_{wd}) to 1%.

Simulations

Four different batch cooling crystallization processes are simulated:

Case 1. Primary and secondary nucleation, unseeded solution
Case 2. Primary and secondary nucleation, seeded solution
Case 3. Primary nucleation but negligible secondary nucleation ($B_s = 0$), unseeded solution
Case 4. Secondary nucleation but negligible primary nucleation ($B_p = 0$), seeded solution.

Linear cooling is used in all simulations, and in the case of seeding, seed crystals are added at time $t = 0$. Process parameters are given in Table 2.

Three different functions for the growth rate distribution are evaluated: a gamma distribution, a log-normal distribution, and a normal distribution. All three functions have been used to fit experimentally-determined growth rate distribution data: gamma distribution (Berglund and Larson, 1984; Liang et al., 1987a,b; Garside and Ristic, 1983); log-normal distribution (Garside and Ristic, 1983); and normal distribution (Liang et al., 1987a,b). The equations are two-parameter distributions, fully defined by specifying the mean and variance. The arithmetic mean growth rate activity, $\bar{k}_g$, is assumed constant, and the influence of the coefficient of variation, CV_g, is examined. The growth rate activity distributions, together with their moments, and the corresponding population density distributions of a subpopulation, Eq. 17, are given in the Appendix. Equal dispersion is assigned to seed crystals and nucleated crystals. From a mathematical point of view, all three distributions are comparable in the model. However, the normal distribution includes negative growth rates to an insignificant extent at low CV_g but of growing importance at increasing coefficient of variation. At $\bar{k}_g$ used in this study, a few percent of the particles receive a negative growth rate at $CV_g = 50\%$. The gamma and log-normal distributions are both confined to the positive range, if appropriate parameter values are used.

The numerical values of the kinetic constants used in the simulations are given in Table 2. Citric acid monohydrate is used as a model substance. Some data given in the specified

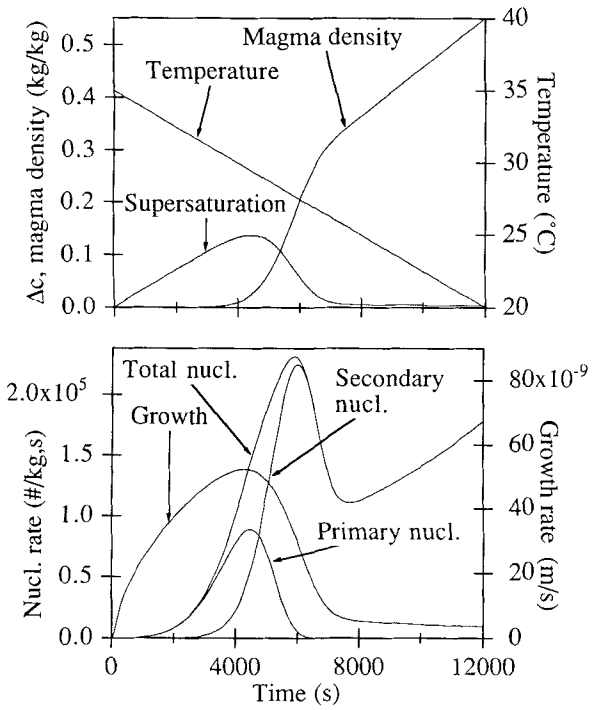

Figure 1. Process information diagrams for a typical simulation.

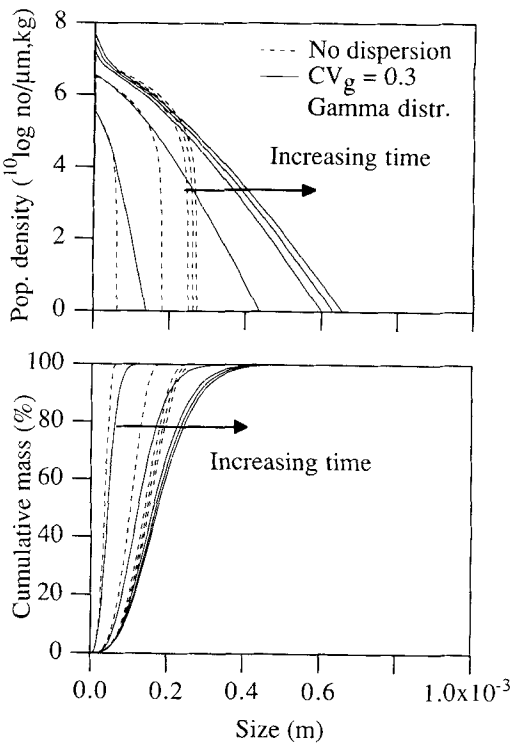

Figure 2. Influence of growth rate dispersion on the evolution of the size distribution: process case 1.

references are transformed before use. This includes recalculating the primary nucleation constant from mass basis to number basis and replacing the dependency of secondary nucleation on the fourth moment by a corresponding dependency on the third moment. It may be questioned whether the adopted kinetics do represent a "normal" case. In particular, the growth rate kinetics (from Sikdar and Randolph, 1976) show a weaker dependency on supersaturation ($g = 0.65$) than is normally observed. By using the data of Ramanarayanan et al. (1985), another set of growth kinetics may be extracted: $\overline{k}_g = 1.9377 \times 10^{-6}$ and $g = 1.65$. All simulations of case 1 have been repeated with these data. The weight mean size and coefficient of variation of the mass distribution are almost identical with the results presented below based on the constants in Table 2. The main difference is found in the number mean size which generally decreases with about 30%. However, the principal influence of growth rate dispersion in Figures 2–5 is unaffected.

Results and Discussion

The complete result from a simulation includes important process information such as the temperature, supersaturation, nucleation rate, growth rate and magma density vs. time. The cumulative mass distribution, the population density distribution, the distribution mean sizes, and coefficient of variations (CV_{nd} and CV_{wd}) are also calculated (Bohlin and Rasmuson, 1990). Below, the presentation is confined to size distributions, product mean size, and coefficient of variation. However, a typical example of the supersaturation and nucleation curves is presented in Figure 1, showing the feature of a supersaturation peak producing a peak in the nucleation rate. In this respect, the analyzed process represents a common batch cooling crystallization.

Influence of growth rate dispersion

The evolution of the population density distribution and cumulative mass distribution for an unseeded process (case 1) with and without dispersion is shown in Figure 2. In the absence of growth rate dispersion (as well as size-dependent growth and size-distributed nucleation), the population density is determined only by the conditions at the moment of birth. The distribution is shifted toward larger sizes, unchanged in shape. In the case of growth dispersion, the population density changes during the growth period, and thus the shape of the curve is gradually changed. In comparison with the nondispersed case, the population density at both large and near-zero sizes increases, while it decreases somewhat in the intermediate region. The distribution becomes wider. Also the cumulative mass distribution becomes considerably wider, because a large proportion of the mass is allocated to larger sizes.

Figure 3 shows the final population density and cumulative undersize mass distributions of an unseeded solution (case 1), resulting from different growth rate activity distribution functions and CV_g. For low CV_g values, the large-size region of the population density curves is somewhat extended, but the influence of growth rate distribution function is negligible. At a CV_g value of 50%, growth dispersion has a significant influence on the crystal-size distributions. The product contains a significant amount of large crystals, and both the cumulative mass and population density distributions become wider. Also, an influence of the particular dispersion function develops. The log-normal distribution alters the population density curve into a concave shape in the upper region and the gamma distribution produces a linear curve. Both of these curves actually bear a close resemblance to distributions from MSMPR crys-

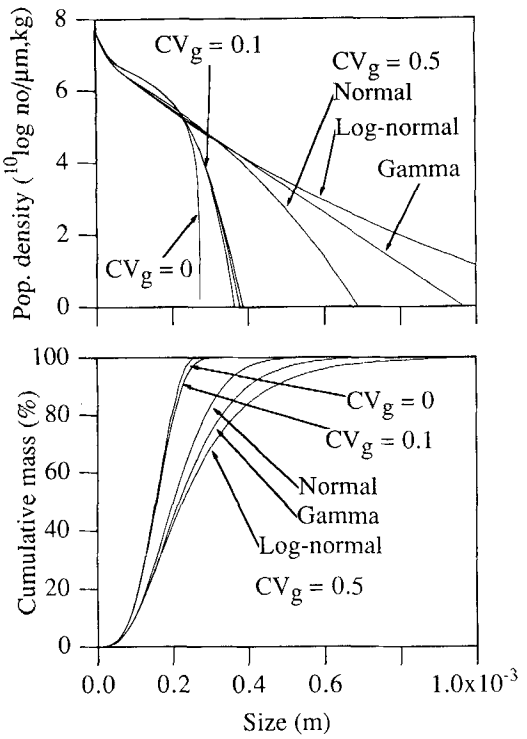

Figure 3. Influence of growth rate activity function and coefficient of variation on product-size distribution: process case 1.

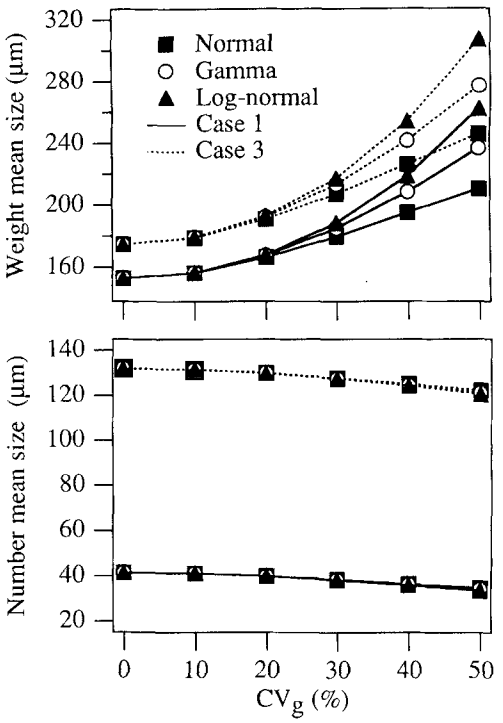

Figure 4. Influence of growth rate activity function and coefficient of variation on product weight and number mean size: process cases 1 and 3.

tallizers. With the normal distribution, the original convex shape of the leading front is still retained at $CV_g = 50\%$, but at even higher dispersion nearly linear population plots are eventually created.

In Figures 4 and 5, the product weight mean size and corresponding coefficient of variation for process cases 1 and 3 are plotted for increasing CV_g and different distribution functions. Both the weight mean size and CV_{wd} increase significantly with increasing CV_g, and an influence of the particular growth dispersion function develops at high CV_g. Figures 4 and 5 also show that the influence on the product number mean size and coefficient of variation is much weaker and for the number mean even slightly reversed. The influence of dispersion function on the number mean size and CV_{nd} is insignificant. In comparison to the above-discussed results, Larson et al. (1985) concluded that in a continuous process the influence of the particular dispersion function on the population density distribution is still insignificant at a CV_g value of 100%.

The observed influence of CV_g and particular dispersion function is the result of two main effects. (i) Increasing dispersion and skewness of the growth rate distribution (normal < gamma < log-normal) directly result in higher values of the second, third and fourth moments (but equal first moments) of the growth rate activity distribution, and thus in a corresponding increase of the moments of the subpopulations. If the supersaturation is constant, the result of increasing dispersion would be a higher weight, but a constant number, mean size of the subpopulations as well as of the total distribution. (ii) Due to the increasing crystal surface area (higher second moments), however, the consumption of supersaturation increases, and both the linear growth rate and the nucleation rate decrease at increasing dispersion (this can be seen in the complete process diagrams). The decrease in the growth rate is dominant in these examples, and therefore, the number mean size decreases. The change in the growth rate, however, is not strong enough to counteract the anticipated increase of the weight mean size or to influence the mass distribution significantly. The influence on the coefficient of variation is more complex. As expected, the standard deviation (σ_{nd} and σ_{wd}) increases in all cases at increasing dispersion. However, since also the mean size changes, the coefficient of variation (CV_{nd} and CV_{wd}) may increase as in Figure 5 or even decrease as in Figure 9 for seeded solutions.

The evolution in time of the population density and cumulative mass distribution in a seeded process with considerable nucleation is shown in Figure 6. Without growth rate dispersion, the seed pulse (here represented by a vertical line of arbitrary height) remains monosized and isolated from the nucleated crystals. In the presence of dispersion ($CV_g = 30\%$), both the seeded and the nucleated distributions continuously become wider and merge. Figure 7 shows the influence of CV_g and growth activity distribution on the product distribution of a seeded process. At $CV_g = 50\%$, it is impossible to distinguish the original seed population from the nucleated crystals in the product, and a strong effect of the particular dispersion function develops. These product distributions resemble those of the unseeded process, Figure 3, and the influence of growth activity distribution function is similar. Obviously, a rather moderate dispersion is sufficient for the otherwise strongly bimodal character of the product of a seeded process to vanish. Size-dependent growth cannot create this effect. Size dependency in itself cannot generate a distribution and only expands a distribution due to, for instance, a distribution of birth times.

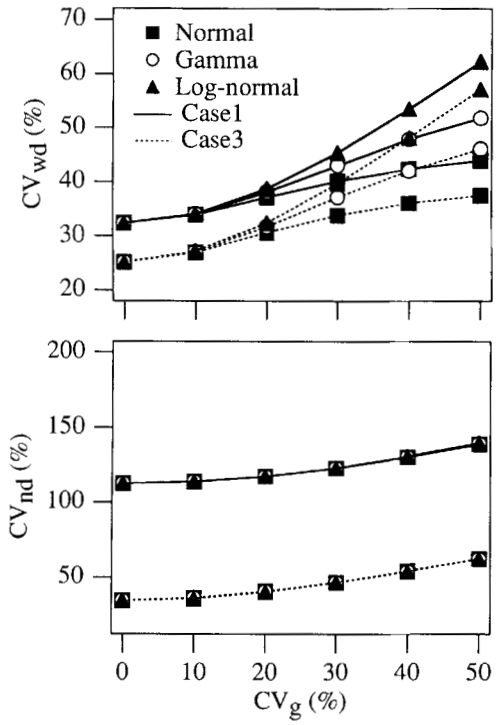

Figure 5. Influence of growth rate activity function and coefficient of variation on product coefficient of variation on mass and number basis: process cases 1 and 3.

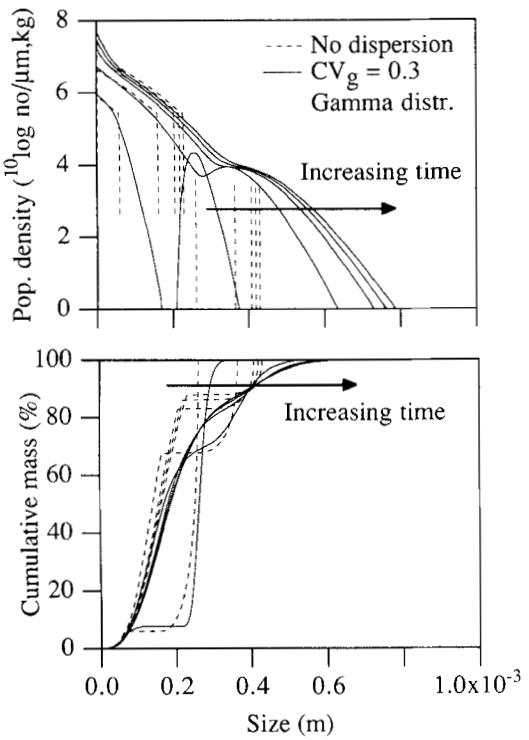

Figure 6. Influence of growth rate dispersion on the evolution of the size distribution: process case 2.

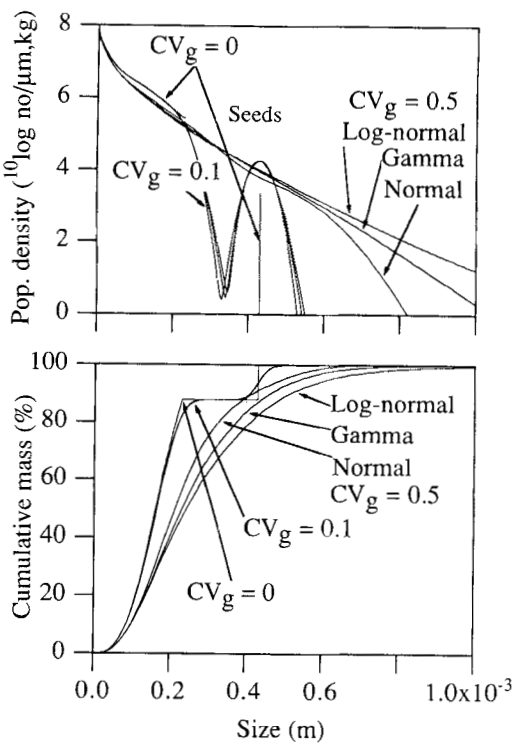

Figure 7. Influence of growth rate activity function and coefficient of variation on product size distribution: process case 2.

White and Wright (1971) observed the broadening of a narrowly-sized crop of seeds growing in a batch crystallizer and suggested the random fluctuation (RF) behavior. As expected and shown in Figure 7, the CCG mechanism widens the seed population in a similar fashion.

The influence of growth distribution function and CV_g value on the product mean values in a seeded process, Figure 8, resembles that of an unseeded process. However, the influence on the weight distribution coefficient of variation (Figure 9) is somewhat different. CV_{wd} is high for a seeded process with secondary nucleation even without dispersion, since the product-size distribution becomes strongly bimodal. It is composed of nucleated crystals and seeded crystals, each type more or less occupying separate distributions. The relative influence of dispersion on CV_{wd} is thus rather limited even at high dispersion. However, since dispersion does have a strong influence on the shape of the product distribution, as shown by Figures 6 and 7, it merely indicates that these distributions are insufficiently characterized by mean size and CV only. Furthermore, Figure 9 shows that CV_{wd} does not always increase with increasing dispersion, although the standard deviation, σ_{wd}, does. This result is also related to the complexity of these distributions. Both the location of the nucleated and seeded distributions (along the size scale), as well as the distribution of the total mass between them, influence the overall CV_{wd}. We conclude that growth dispersion may have a strong influence on the product also in the case of a seeded process.

The model

As opposed to previous modeling (Shiau and Berglund, 1990;

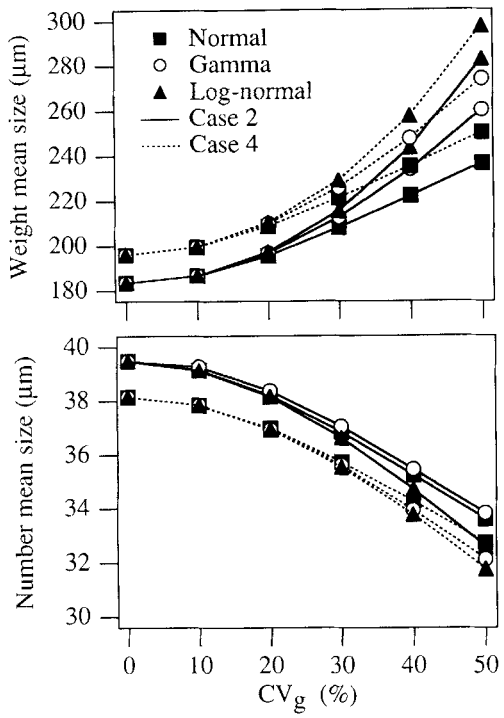

Figure 8. Influence of growth rate activity function and coefficient of variation on product weight and number mean size: process cases 2 and 4.

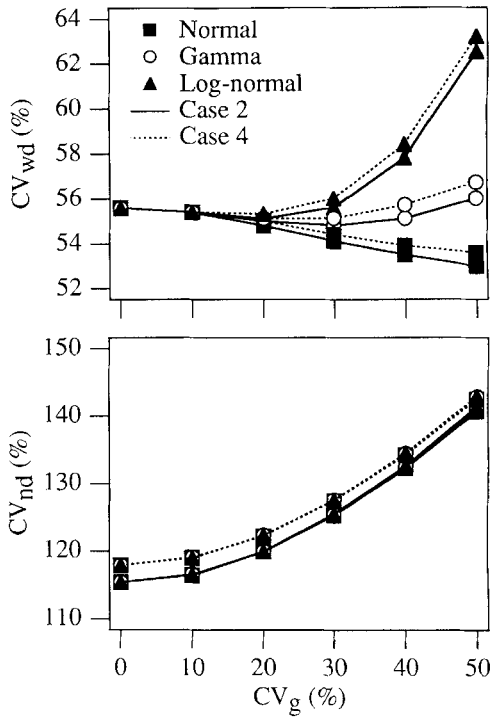

Figure 9. Influence of growth rate activity function and coefficient of variation on product coefficient of variation on mass and number basis: process cases 2 and 4.

Klug and Pigford, 1989), the proposed method recovers the entire size distribution, not just moments. This is especially of importance when primary and secondary nucleation proceed during the whole process, or seeding is used and secondary nucleation occurs. In both cases, the resulting product-size distribution may become irregular and is not sufficiently characterized by the first moments alone (that is, mean size and standard deviation).

Janse (1977) and de Jong (1986) use a method having the same basic approach as the one presented in this article. However, instead of calculating the moments of the subpopulations, the growth rate activity distribution is discretized into a number of growth rate classes, and each new pulse of crystals is separated into the corresponding number of subpopulations. Then, Eq. 4 is solved for each growth rate class, and the total distribution is the sum of the result of all growth classes. Unfortunately, with a certain number of growth rate groups and at the same mean growth activity and variance, the discretization of the growth rate distribution may be done differently in terms of boundaries and representation of each group. This introduces an ambiguity concerning the actual dispersion at hand and complicates the comparison of different dispersion cases. Furthermore, the method requires considerably longer computing times.

In accordance with the model of Klug and Pigford (1989), we assume $\bar{k}_g$ and CV_g to be independent of supersaturation. However, a dependence of both variables on the supersaturation prevailing at the moment of birth can be accounted for in the model by assigning individual values on $\bar{k}_g$ and CV_g to each subpopulation. Seed crystals can be assigned dispersion characteristics, separate from those of nucleated crystals.

Conclusions

A series of computer simulations of batch cooling crystallization is presented for a model substance using kinetics from the literature. The crystallization model accounts for primary and magma density-dependent secondary nucleation and growth rate dispersion of the constant crystal growth type. The model is solved by a combination of the method of characteristics and moment analysis, by which the entire product-size distribution is recovered. Unseeded and seeded processes are analyzed. The simulations of this study show that growth rate dispersion may exhibit a strong influence on the product of a batch cooling crystallizer. For the particular unseeded cases studied, a significant increase in the coefficient of variation of the product weight size distribution arises already at moderate growth dispersion ($CV_g = 30\%$). There is also an increase of the product weight mean size at increasing growth dispersion. At high dispersion, ($CV_g = 50\%$), there is an important influence of the actual shape of the growth rate activity distribution. The strongest influence on the product arises when the growth distribution is a log-normal distribution, a somewhat less strong influence if it follows a gamma distribution and the weakest influence arises from a normal distributed growth dispersion. For the seeded cases of the study, the influence of growth dispersion on the product weight mean size is comparable to the unseeded cases. The coefficient of variation of the weight distribution, however, is high for a seeded process even without dispersion and the relative influence of dispersion becomes limited. However, the actual shape of the size distribution is strongly influenced. The bimodal character is efficiently smoothed out already at moderate dispersion.

Acknowledgment

The financial support of The Swedish Board for Technical Development (STU), The Swedish Council for Planning and Coordination of Research (FRN), and The Swedish Industrial Association for Crystallization Research and Development (IKF) are gratefully acknowledged.

Notation

a = parameter in gamma distribution
b = parameter in gamma distribution
b = empirical mass exponent
B_p = primary nucleation rate, no/s/kg H_2O
B_s = secondary nucleation rate, no/s/kg H_2O
c^* = equilibrium concentration, kg/kg H_2O
c_o = constant, kg/kg H_2O
c_1 = constant, kg/kg H_2O/°C
c_2 = constant, kg/kg H_2O/(°C)^2
c_3 = constant, kg/kg H_2O/(°C)^3
Δc = supersaturation, kg/kg H_2O
Δc_o = initial supersaturation, kg/kg H_2O
CV = coefficient of variation, $CV = \sigma/\bar{x}$
D = driving force function, (kg/kg)^g
G = linear growth rate, m/s
g = growth rate order
k = number of subpopulations
k_g = growth rate activity, m/s (kg/kg)$^{-g}$
k_p = primary nucleation rate constant, no/kg (kg/kg)$^{-n_p}$
k_s = secondary nucleation rate constant, no/kg (kg/kg)$^{-n_s-b}$
k_v = volume shape factor
L = characteristic crystal dimension, m
L_{io} = initial size of ith subpopulation, m
m = moment or mass of distribution
m_{cum} = cumulative undersize mass
m_{gr} = rth moment of growth rate activity distribution
m_{Lj} = jth moment of total size distribution
m_{Lji} = jth moment of ith subpopulation size distribution
M = mass of solvent, kg
M_o = initial mass of solvent, kg
n = population density, no/kg/m
n_p = primary nucleation rate exponent
n_s = secondary nucleation rate exponent
N = number of crystals in pulse, no/kg
P = growth rate activity or size distribution function
R = ratio of molecular weights of hydrous and anhydrous salt
Δt = time interval, s
t = time, s
t_i = birth time of pulse, s
t_f = total batch time, s
T = temperature, K
W_T = suspended solids concentration, kg hydrate/kg H_2O

Greek letters

α = parameter in gamma distribution
β = parameter in gamma distribution
Γ = Gamma function
Θ = transformed time, (kg/kg)^g·s
θ_f = final temperature, °C
θ_o = initial temperature, °C
ρ_c = density of crystals, kg/m^3
σ = standard deviation

Superscripts

~ = variable expressing total amount in whole crystallizer
— = mean value of variable

Subscripts

g = growth rate activity distribution
G = growth rate distribution
i = variable related to subpopulation born at time t_i
L = size distribution
nd = number distribution
s = seed
wd = weight distribution

Literature Cited

Allen, T., *Particle Size Measurement*, 3rd ed., Chapman and Hall, London (1981).
Berglund, K. A., "Formation and Growth of Contact Nuclei," PhD Diss., Iowa State Univ. of Science and Technology, Ames, IA (1981).
Berglund, K. A., E. L. Kaufman, and M. A. Larson, "Growth of Contact Nuclei of Potassium Nitrate," *AIChE J.*, **29**, 867 (1983).
Berglund, K. A., and M. A. Larson, "Growth of Contact Nuclei of Citric Acid Monohydrate," *AIChE Symp. Ser.*, **78**, 9 (1982).
Berglund, K. A., and M. A. Larson, "Modeling of Growth Rate Dispersion of Citric Acid Monohydrate in Continuous Crystallizers," *AIChE J.*, **30**, 280 (1984).
Berglund, K. A., and V. G. Murphy, "Modeling Growth Rate Dispersion in a Batch Sucrose Crystallizer," *Ind. Eng. Chem. Fundam.*, **25**, 174 (1986).
Blem, K. E., and K. A. Ramanarayanan, "Generation and Growth of Secondary Ammonium Dihydrogen Phosphate Nuclei," *AIChE J.*, **33**, 677 (1987).
Bohlin, M., and Å. C. Rasmuson, "Computer Analysis of Batch Cooling Crystallization," *Symp. Industrial Crystallization*, A. Mersmann, ed., p. 23 (1990).
Bohlin, M., and Å. C. Rasmuson, "Application of Controlled Cooling and Seeding in Batch Crystallization," *Can. J. Chem. Eng.*, **70**, 120 (1992).
Garside, J., and R. I. Ristic, "Growth Rate Dispersion Among ADP Crystals Formed by Primary Nucleation," *J. Cryst. Growth*, **61**, 215 (1983).
Gupta, B. S., and T. K. Dutta, "Growth Rate Dispersion in a Continuous Sucrose Crystallizer and its Effect on CSD," *Chem. Eng. Technol.*, **13**, 196 (1990).
Human, H. J., and W. J. P. van Enckevort, and P. Bennema, "Spread in Growth Rates of the {111}, {100} Faces of Potash Alum Growing From Aqueous Solution," *Industrial Crystallization*, S. J. Jancic and E. J. de Jong, eds., p. 387, North-Holland Pub. Co., Amsterdam (1982).
Jager, J., S. de Wolf, H. J. M. Kramer, and E. J. de Jong, "Estimation of Nucleation Kinetics from Crystal Size Distribution Transients of a Continuous Crystallizer," *Chem. Eng. Sci.*, **47**, 807 (1991).
Janse, A. H., "Nucleation and Crystal Growth in Batch Crystallizers," PhD Thesis, The Netherlands Univ. of Technology, Delft (1977).
Janse, A. H., and E. J. de Jong, "Growth and Growth Rate Dispersion," *Industrial Crystallization*, E. J. de Jong and S. J. Jancic, eds., p. 135, North-Holland Pub. Co., Amsterdam (1979).
Janse, A. H., and E. J. de Jong, "The Occurrence of Growth Dispersion and Its Consequences," *Industrial Crystallization*, J. W. Mullin, ed., p. 145, Plenum Press, New York (1976).
de Jong, E. J., "Computer Control of Industrial Crystallizers," *World Cong. III of Chem. Eng.*, Tokyo, p. 1080 (1986).
Klug, D. L., and R. L. Pigford, "The Probability Distribution of Growth Rates of Anhydrous Sodium Sulfate Crystals," *Ind. Eng. Chem. Res.*, **28**, 1718 (1989).
Kramer, H. J. M., S. de Wolf, and J. Jager, "Simulation of the Dynamic Behavior of Continuous Crystallizers," *Crystallization as a Separation Process*, ACS Symp. Ser. No. 438, A. S. Meyerson, and K. Toyokura, eds. (1990).
Laguerie, C., and H. Angelino, "Determination of Crystal Growth Rates," *Industrial Crystallization*, E. J. de Jong and S. J. Jancic, eds., p. 377, North Holland Pub. Co., Amsterdam (1979).
Lakatos, B., E. Varga, S. Halasz, and T. Blickle, "Simulation of Batch Crystallizers," *Industrial Crystallization*, S. J. Jancic and E. J. de Jong, eds., p. 185, Elsevier Science, Amsterdam (1984).
Larson, M. A., E. T. White, K. A. Ramanarayanan, and K. A. Berglund, "Growth Rate Dispersion in MSMPR Crystallizers," *AIChE J.*, **31**, 90 (1985).
Liang, B. M., R. W. Hartel, and K. A. Berglund, "Contact Nucleation in Sucrose Crystallization," *Chem. Eng. Sci.*, **42**, 2723 (1987a).
Liang, B. M., R. W. Hartel, and K. A. Berglund, "Growth Rate

Dispersion in Seeded Batch Sucrose Crystallization," *AIChE J.*, **33**, 2077 (1987b).
Mathis-Lilley, J. J., and K. A. Berglund, "Contact Nucleation From Aqueous Potash Alum Solutions," *AIChE J.*, **31**, 865 (1985).
Melikhov, I. V., and L. B. Berliner, "Simulation of Batch Crystallization," *Chem. Eng. Sci.*, **36**, 1021 (1981).
Mukhopadhyay, S. C., and M. A. Epstein, "Computer Model for Crystal Size Distribution Control in a Semi-Batch Evaporative Crystallizer," *Ind. Eng. Chem. Process Des. Dev.*, **19**, 352 (1980).
Mullin, J. W., *Crystallization*, 2nd ed., Butterworks, London (1972).
Nyvlt, J., O. Söhnel, M. Matuchova, and M. Broul, *The Kinetics of Industrial Crystallization*, Chemical Engineering Monographs 19, Elsevier, Amsterdam (1985).
Qiu, Y., and Å. C. Rasmuson, "Nucleation and Growth of Succinic Acid in a Batch Cooling Crystallizer," *AIChE J.*, **37**, 1293 (1991).
Ramanarayanan, K. A., M. A. Athreya, and M. A. Larson, "Statistical-Mathematical Modeling of CSD in Continuous and Batch Crystallizers," *AIChE Symp. Ser.*, **80**, 76 (1984).
Ramanarayanan, K. A., K. A. Berglund, and M. A. Larson, "Growth Kinetics in the Presence of Growth Rate Dispersion from Batch Crystallizers," *Chem. Eng. Sci.*, **40**, 1604 (1985).
Randolph, A. D., and E. T. White, "Modeling Size Dispersion in the Prediction of Crystal-Size Distribution," *Chem. Eng. Sci.*, **32**, 1067 (1977).
Randolph, A. D., and M. A. Larson, *Theory of Particulate Processes*, 2nd ed., Academic Press, New York (1988).
Rousseau, R. W., and R. C. Zumstein, "The Influence of Growth Rate Dispersion on Crystal Size Distributions," *World Cong. III of Chem. Eng.*, Tokyo, 1064 (1986).
Shiau, L., and K. A. Berglund, "Growth Kinetics of Fructose Crystals Formed by Contact Nucleation," *AIChE J.*, **33**, 1028 (1987).
Shiau, L., and K. A. Berglund, "Growth Rate Dispersion in Batch Crystallizers," *AIChE J.*, **36**, 1669 (1990).
Sikdar, S. K., and A. D. Randolph, "Secondary Nucleation of Two Fast Growth Systems in a Mixed Suspension Crystallizer: Magnesium Sulfate and Citric Acid Water Systems," *AIChE J.*, **22**, 110 (1976).
Tavare, N. S., and J. Garside, "The Characterization of Growth Dispersion," *Industrial Crystallization*, S. J. Jancic and E. J. de Jong, eds., p. 21. North-Holland Pub. Co., Amsterdam (1982).
Tavare, N. S., "Batch Crystallizers: A Review," *Chem. Eng. Comm.*, **61**, 259 (1987).
Tulke, A., and H. Offerman, "The Problem of Growth Rate Dispersion," *Symp. of Industrial Crystallization*, A. Mersmann, ed., p. 441 (1990).
Zumstein, R. C., and R. W. Rousseau, "Growth Rate Dispersion in Batch Crystallization with Transient Conditions," *AIChE J.*, **33**, 1921 (1987).
White, E. T., and P. G. Wright, "Magnitude of Size Dispersion Effects in Crystallization," *Chem. Eng. Symp. Ser.*, **67**, 81 (1971).

Appendix

Growth rate activity distribution functions correspond to size distribution functions given by Randolph and Larson (1988). The corresponding subpopulation density distributions admit a possible initial size, L_{io}, of each subpopulation. In our simulations, only the seeds have an initial size larger than zero. All distribution functions (P_{gi} and P_{Li}) are normalized: $m_{goi} = m_{Loi} = 1$.

Normal distribution:

$$P_g = \frac{1}{\sqrt{2\cdot\pi}\ \sigma_g} \exp\left[\frac{-(k_g-\bar{k}_g)^2}{2\cdot\sigma_g^2}\right] \tag{A1}$$

$$m_{g0} = 1 \tag{A2}$$

$$m_{g1} = \bar{k}_g \tag{A3}$$

$$m_{g2} = \bar{k}_g^2 + \sigma_g^2 \tag{A4}$$

$$m_{g3} = \bar{k}_g^3 + 3\cdot\bar{k}_g\cdot\sigma_g^2 \tag{A5}$$

$$m_{g4} = \bar{k}_g^4 + 6\cdot\bar{k}_g^2\cdot\sigma_g^2 + 3\cdot\sigma_g^4 \tag{A6}$$

$$m_{g5} = \bar{k}_g^5 + 10\cdot\bar{k}_g^3\cdot\sigma_g^2 + 15\cdot\sigma_g^4\cdot\bar{k}_g \tag{A7}$$

$$\tilde{n}_i(L) = \tilde{N}_i\cdot P_{Li} = \tilde{N}_i\cdot\frac{1}{\sqrt{2\cdot\pi}\ \sigma_{Li}} \exp\left[\frac{-[(L-L_{io})-(\bar{L}_i-L_{io})]^2}{2\cdot\sigma_{Li}^2}\right] \tag{A8}$$

Note that the normal distribution is independent of the initial size (L_{io} vanishes) and the population density below the initial size is not zero.

Gamma distribution:

$$P_g = \frac{1}{\Gamma(a+1)b^{a+1}}\, k_g^a \exp\left[-\frac{k_g}{b}\right] \tag{A9}$$

$$a = \frac{\bar{k}_g^2}{\sigma_g^2} - 1 = \frac{1}{CV_g^2} - 1 \tag{A10}$$

$$b = \frac{\bar{k}_g}{a+1} \tag{A11}$$

$$m_{gj} = b^j\Gamma(a+j+1)/\Gamma(a+1) \tag{A12}$$

$$\tilde{n}_i(L) = \tilde{N}_i\cdot P_{Li} = \tilde{N}_i\cdot\frac{1}{\Gamma(\alpha+1)\beta^{\alpha+1}}\,[L-L_{io}]^{\alpha}\exp\left[-\frac{[L-L_{io}]}{\beta}\right] \tag{A13}$$

where $L \geq L_{io}$. It may be shown by integration that the parameters α and β are defined as:

$$\alpha = \frac{[\bar{L}_i-L_{io}]^2}{\sigma^2_{Li}} - 1 \tag{A14}$$

$$\beta = \frac{[\bar{L}_i-L_{io}]}{\alpha+1} \tag{A15}$$

Log-normal distribution:

$$P_g = \frac{1}{\sqrt{2\cdot\pi}\ \ln\sigma_g'} \exp\left[-\frac{[\ln k_g - \ln\bar{k}_g']^2}{2\cdot\ln^2\sigma_g'}\right] \tag{A16}$$

$$\bar{k}_g' = \frac{\bar{k}_g}{\exp[0.5\ln^2\sigma_g']} \tag{A17}$$

$$\ln\sigma_g' = \sqrt{\ln(CV_g^2+1)} \tag{A18}$$

$$m_j = \bar{k}_g'^{\,j}\cdot\exp[0.5\cdot j^2\ln^2\sigma_g'] \tag{A19}$$

$$\tilde{n}(L) = \tilde{N}_i \cdot \frac{1}{\sqrt{2 \cdot \pi}\, \ln\sigma'_{Li}} \cdot \frac{1}{(L - L_{io})} \cdot \exp\left[-\frac{[\ln(L - L_{io}) - \ln\bar{L}'_i]^2}{2 \cdot \ln^2\sigma'_{Li}} \right] \quad \text{(A20)}$$

where $L \geq L_{io}$. The population densities from the log-normal distribution are here converted from (no/log m, kg) to (no/m, kg) by the factor $1/(L - L_{io})$ (Allen, 1981). The relation between the two parameters characterizing the distribution and the mean and variance can be shown to be:

$$\bar{L}'_i = \frac{\bar{L}_i - L_{io}}{\exp[0.5 \ln^2\sigma'_{Li}]} \quad \text{(A21)}$$

$$\ln\sigma'_{Li} = \sqrt{\ln\left(\left(\frac{\sigma_{Li}}{\bar{L}_i - L_{io}}\right)^2 + 1\right)} \quad \text{(A22)}$$

Manuscript received Dec. 2, 1991, and revision received June 22, 1992.